ADAPTIVE FINITE ELEMENT FREQUENCY DOMAIN METHOD FOR EDDY CURRENT PROBLEMS *

WEIYING ZHENG † AND FEIRAN ZHANG‡

Abstract. In the present paper, adaptive finite element methods are studied for time-harmonic eddy current problems in the case of three-dimensional isotropic and linear materials. We adopt the formulation based-on the magnetic field and a magnetic scalar potential in this paper, since it needs the least number of unknowns. Reliable and efficient a posteriori error estimates are obtained and the efficiency of the adaptive algorithm is demonstrated by numerical and engineering experiments.

Key words. Time-harmonic Maxwell's equations, eddy current, adaptive finite element method, multiply connected domain

AMS subject classifications. 65M60, 65M50, 78A25

1. Introduction.

Eddy currents appear in almost all electromagnetic devices. They cause energy loss and may reduce lifespan of devices. The three-dimensional eddy current problem is an approximate model which describes very low-frequency electromagnetic phenomena. In this case, displacement currents may be neglected (see [1] and [5, Ch. 8]). The time-harmonic Maxwell equations read (see [1] and [5, Ch. 8]):

$$\mathbf{curl}\,\mathbf{H} - \sigma\mathbf{E} - \mathbf{J}_s = \mathbf{0} \quad \text{in} \quad \mathbb{R}^3, \tag{1.1a}$$

$$\mathbf{i}\,\omega\,\mu\,\mathbf{H} + \mathbf{curl}\,\mathbf{E} = \mathbf{0} \quad \text{in} \quad \mathbb{R}^3, \tag{1.1b}$$

$$\mathrm{div}(\mu\mathbf{H}) = 0 \quad \text{in} \quad \mathbb{R}^3, \tag{1.1c}$$

where $\mathbf{E}$ is the electric field, $\mathbf{H}$ is the magnetic field, $\mathbf{J}_s$ is the source current density carried by some coils, $\mathbf{i}$ is the imaginary unit, ω is angular frequency, μ is the magnetic permeability, and σ is the electric conductivity of the material and is only nonzero in conducting regions.

The system (1.1) may be simplified into different forms by virtue of various field variables (see [15] and references therein). Generally speaking, each of these simplified formulations contains at least an unknown vector function defined in the conducting region, plus an unknown vector function or an unknown scalar function defined in the nonconducting region. From the point of view of numerical computation, the latter case needs less degrees of freedom and thus is more favorable. In this paper, we adopt a formulation based on the magnetic field $\mathbf{H}$ in the conducting region, denoted by Ω_c, and the magnetic scalar potential ψ in the nonconducting region, denoted by $\mathbb{R}^3 \setminus \overline{\Omega_c}$. When all connected components of the conducting region are simply connected, the scalar potential ψ belongs to $H^1(\mathbb{R}^3 \setminus \overline{\Omega_c})$ and the problem is relatively easy to deal with in the framework of finite element method. Otherwise, in the case of multiply connected conductors, ψ is discontinuous somewhere in the nonconducting region (see [2] and [25]) and thus the problem becomes more difficult. We focus on this case and treat the discontinuities of ψ by making "cuts" in the nonconducting region.

*This work was supported by the National Natural Foundation of China 10401040.

†LSEC, Institute of Computational Mathematics, Academy of Mathematics and System Sciences, Chinese Academy of Sciences, Beijing, 100080, People's Republic of China (zwy@lsec.cc.ac.cn).

‡Department of Mathematics, Shangqiu Teacher's College, Shangqiu 476000, People's Republic of China (zhangfeiran666@sina.com).

The eddy current limit and the singularities of the solution were discussed in [14] and [1]. Clemens investigated the finite integral method for eddy current problems [13]. In fact, the finite element method is one of the most popular methods in computational electromagnetics (see [5, Ch.8], [6], and references therein).

The adaptive finite element method is one of most efficient numerical methods. Based on mathematically rigorous a posteriori error estimates, it equidistributes the error and may produces quasi-optimal meshes [9] [24] . A posteriori error estimates are computable quantities in terms of the discrete solution and known datum that measure the actual discretization errors without the knowledge of the exact solution. Ever since the pioneering work of Babuška and Rheinboldt [3], adaptive finite element methods based on a posteriori error estimates have become a central theme in scientific and engineering computing. The ability to control error and the asymptotically optimal approximation property (see e.g. [7], [18], and [12]) make the adaptive finite element method attractive for complicated physical and industrial processes (cf. e.g. [8] and [10]).

Adaptive finite element methods for electromagnetic problems were investigated by Monk for Maxwell scattering problems [17], Beck and etc for the electric field-based formulation of eddy current problems [4], Zheng and etc for time-dependent eddy current problems [25], Chen and etc for time-harmonic Maxwell's equations with singularities [11]. Recently, Sterz et al. investigated the adaptive local multigrid method for time-harmonic eddy-current problems based on the formula of electric field [23].

In this paper, we focus on time-harmonic eddy current problems. They are frequently used in practice, since most source fields are periodic and also produce periodic electromagnetic fields. Furthermore, this model comprises almost all difficulties of linear eddy current problems, except for the iterations in the time direction. We develop an adaptive finite element method based on reliable and efficient a posteriori error estimates for eddy current problems in multiply connected conductors.

To show the competitive performance of our method, we compute two challenging numerical experiments. One is an engineering benchmark problem, the Team Workshop Problem 7, and the other has analytic solution. The results indicate that our adaptive method has the following very desirable quasi-optimality property:

$$\eta_j \approx C\, N_j^{-1/3}$$

is valid asymptotically, where η_j is the error estimate and N_j is the number of elements of the mesh $\mathcal{T}_j$ with j being the level of $\mathcal{T}_j$.

The rest of the paper is arranged as follows: In section 2, we derive the $\mathbf{H}-\psi$ based formulation of time-harmonic eddy current problems. The equivalent weak formulation and its well-posedness are also given in this section. In section 3, we introduce a coupled conforming finite element approximation to the $\mathbf{H}-\psi$ based formulation and prove the Helmholtz decomposition of the variational space. In section 4, we derive reliable and efficient residual-based a posteriori error estimates. In section 5, we report the numerical results for a singular solution and the Team Workshop Problem 7, and compare them with experimental values to show the competitive performance of the method proposed in this paper.

2. Magnetic field and magnetic scalar potential based formulation. Let $\Omega \subset \mathbb{R}^3$ be a sufficiently large and convex polyhedral domain which contains all conductors and coils (see Fig. 2.1 for a typical model with one conductor and one coil). Denote the conducting domain by Ω_c which consists of all conductors and the

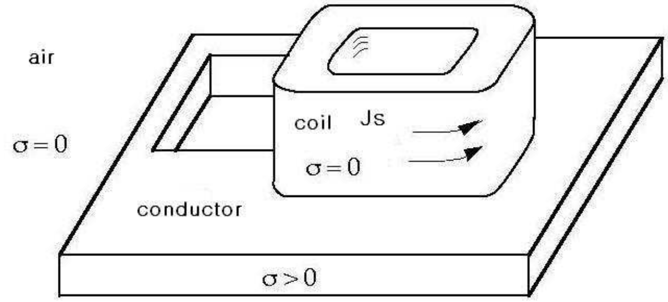

FIG. 2.1. *Team Problem 7: A conductor with a hole.*

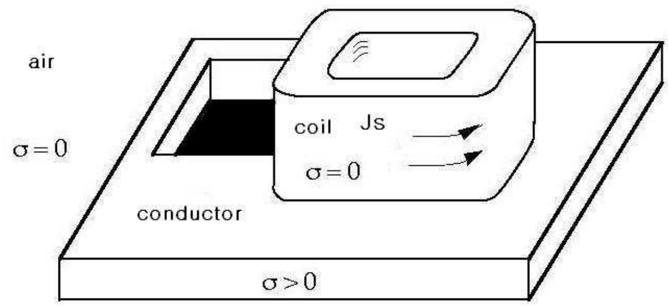

FIG. 2.2. *Team Problem 7: Cover the hole by making "cut".*

nonconducting domain by $\Omega \setminus \overline{\Omega_c}$. We assume that Ω_c is bounded and each of its connected components has connected Lipschitz-continuous boundary. Furthermore, we assume there exist I surfaces Σ_i, $1 \le i \le I$, called "cuts", such that (see Fig. 2.2 for $I = 1$)

- each cut Σ_i is an open part of some smooth two-dimensional manifold with Lipschitz-continuous boundary, $i = 1, \cdots, I$,
- the boundary of Σ_i is contained in $\partial\Omega_c$ and $\overline{\Sigma}_i \cap \overline{\Sigma}_j = \emptyset$ for $i \neq j$,
- the open set $\Omega_e := (\Omega \setminus \overline{\Omega_c}) \setminus (\cup_{i=1}^{I} \Sigma_i)$ is a simply connected and pseudo-Lipschitz domain (see Definition 3.1 of [2] for the definition of pseudo-Lipschitz domain).

For each Σ_i, we fix its unit normal vector $\boldsymbol{n}$ pointing to one side.

We make the following general assumptions on material parameters:

$\mu(\boldsymbol{x})$ and $\sigma(\boldsymbol{x})$ are all real valued $L^\infty(\Omega)$ functions. There exist positive constants $\mu_{\min}$ and $\sigma_{\min}$ such that $\mu(\boldsymbol{x}) \ge \mu_{\min}$ in Ω and $\sigma(\boldsymbol{x}) \ge \sigma_{\min}$ in Ω_c. $\sigma(\boldsymbol{x}) \equiv 0$ outside of Ω_c.

These assumptions are reasonable since μ and σ are physical parameters.

We introduce some notation and Sobolev spaces used in this paper. Let $L^2(\Omega)$ be the usual Hilbert space of square integrable complex functions equipped with the following inner product and norm:

$$(u,\, v) := \int_\Omega u(\boldsymbol{x})\, \overline{v(\boldsymbol{x})}\, d\boldsymbol{x} \quad \text{and} \quad \|u\|_{0,\Omega} := (u,\, v)^{1/2}.$$

Define

$$H^m(\Omega) := \{v \in L^2(\Omega) \,:\, D^\xi v \in L^2(\Omega),\ |\xi| \le m\}$$

which is equipped with the following norm and semi-norm

$$\|v\|_{m,\Omega} := \left(\sum_{|\xi|\le m} \|D^\xi v\|_{0,\Omega}^2 \right)^{1/2} \quad \text{and} \quad |v|_{m,\Omega} := \left(\sum_{|\xi|= m} \|D^\xi v\|_{0,\Omega}^2 \right)^{1/2},$$

where ξ represents non-negative triple index. As usual, $H_0^1(\Omega)$ is the subspace of $H^1(\Omega)$ whose functions have zero traces on $\partial\Omega$. Further we define

$$H_\Sigma^1(\Omega) := \{v \in H^1(\Omega_e) \,:\, [v]_{\Sigma_j} = \text{const.},\ 1 \le j \le I\},$$

where $[v]_{\Sigma_j} := v|_{\Sigma_j^+} - v|_{\Sigma_j^-}$ is the jump of v across Σ_j. Throughout the paper we denote vector-valued quantities by boldface notation, such as $\mathbf{L}^2(\Omega) := (L^2(\Omega))^3$.

The Hilbert spaces of the rotation operator are defined by

$$\begin{aligned} \mathbf{H}(\mathbf{curl};\Omega) &:= \{\mathbf{v} \in \mathbf{L}^2(\Omega) \,:\, \mathbf{curl}\,\mathbf{v} \in \mathbf{L}^2(\Omega)\}, \\ \mathbf{H}_0(\mathbf{curl};\Omega) &:= \{\mathbf{v} \in \mathbf{H}(\mathbf{curl};\Omega) \,:\, \boldsymbol{n} \times \mathbf{v} = 0 \ \text{ on } \partial\Omega\}. \end{aligned}$$

Here $\mathbf{H}(\mathbf{curl};\Omega)$ and $\mathbf{H}_0(\mathbf{curl};\Omega)$ are equipped with the following norm:

$$\|\mathbf{v}\|_{\mathbf{H}(\mathbf{curl};\Omega)} := \left(\|\mathbf{v}\|_{0,\Omega}^2 + \|\mathbf{curl}\,\mathbf{v}\|_{0,\Omega}^2\right)^{1/2}.$$

For any $\varphi \in H_\Sigma^1(\Omega_e)$, we can extend $\nabla\varphi \in \mathbf{L}^2(\Omega_e)$ continuously to a function $\tilde{\nabla}\varphi \in \mathbf{L}^2(\Omega \setminus \overline{\Omega_c})$ such that

$$\tilde{\nabla}\varphi = \nabla\varphi, \quad \text{in} \quad \Omega_e\,. \tag{2.1}$$

Lemma 2.1. [2, Lemma 3.11] *Let $\varphi \in H^1(\Omega_e)$. Then $\varphi \in H_\Sigma^1(\Omega_e)$ if and only if*

$$\mathbf{curl}(\tilde{\nabla}\varphi) = 0, \quad \textit{in} \quad \Omega \setminus \overline{\Omega_c}\,. \tag{2.2}$$

With Lemma 2.1, it is easy to show the following lemma.

Lemma 2.2. *For any $\mathbf{v} \in \mathbf{L}^2(\Omega \setminus \overline{\Omega_c})$ satisfying $\mathbf{curl}\,\mathbf{v} = 0$ in $\Omega \setminus \overline{\Omega_c}$, there exists a unique $\varphi \in H_\Sigma^1(\Omega_e)/\mathbb{R}^1$ such that*

$$\mathbf{v} = \tilde{\nabla}\varphi, \quad \textit{in} \quad \Omega \setminus \overline{\Omega_c}\,. \tag{2.3}$$

It is reasonable in practice to assume that $\operatorname{div} \mathbf{J}_s(\boldsymbol{x}) = 0$, then there exists a source magnetic field $\mathbf{H}_s$ such that

$$\mathbf{J}_s = \mathbf{curl}\, \mathbf{H}_s \quad \text{in } \mathbb{R}^3. \tag{2.4}$$

The field $\mathbf{H}_s$ can be constructed explicitly for coils in regular shapes or by the Biot-Savart Law for general coils:

$$\mathbf{H}_s := \mathbf{curl}\, \mathbf{A}_s \quad \text{where} \quad \mathbf{A}_s(\boldsymbol{x}) := \frac{1}{4\pi} \int_{\mathbb{R}^3} \frac{\mathbf{J}_s(\boldsymbol{y})}{|\boldsymbol{x} - \boldsymbol{y}|}\, d\boldsymbol{y}.$$

Define the reaction field by $\mathbf{H}_0 := \mathbf{H} - \mathbf{H}_s$ (see also [16, 25]). By (1.1) and (2.4)), we have

$$\mathbf{curl}\, \mathbf{H}_0 = 0, \quad \text{in } \mathbb{R}^3 \setminus \overline{\Omega_c}\,.$$

We assume the total magnetic field $\mathbf{H} \in \mathbf{L}^2(\mathbb{R}^3)$ because of the finite energy of the field. By Lemma 2.2, there exists a unique potential $\psi \in H^1_\Sigma(\Omega_e)/\mathbb{R}^1$ such that

$$\mathbf{H}_0 = \tilde{\nabla}\psi \quad \text{in } \Omega \setminus \overline{\Omega_c}\,.$$

Since Ω is large enough, we may set the approximate boundary condition by the non-flux condition on $\partial\Omega$:

$$\mu\, \mathbf{H} \cdot \boldsymbol{n} = 0 \quad \text{on } \partial\Omega\,. \tag{2.5}$$

Next we are going to eliminate the electric field $\mathbf{E}$ and derive a weak formulation of (1.1). Since the tangential field $\mathbf{H}_0 \times \boldsymbol{n}$ is continuous across $\partial\Omega_c$, we add this constraint to all test functions and define the test function space by

$$\mathbf{U} = \Big\{ \mathbf{v} :\ \mathbf{v} = \tilde{\nabla}\varphi \ \text{ in } \Omega \setminus \overline{\Omega_c} \text{ and } \mathbf{v} = \mathbf{w} \text{ in } \Omega_c \text{ such that } \nabla\varphi \times \boldsymbol{n} = \mathbf{w} \times \mathbf{n} \text{ on } \partial\Omega_c,$$
$$\varphi \in H^1_\Sigma(\Omega_e)/\mathbb{R}^1 \text{ and } \mathbf{w} \in \mathbf{H}(\mathbf{curl};\, \Omega_c) \Big\}\,.$$

Clearly $\mathbf{U} \subset \mathbf{H}(\mathbf{curl}; \Omega)$ and is equipped with the induced inner product and norm of $\mathbf{H}(\mathbf{curl};\, \Omega)$.

For any $\varphi \in H^1_\Sigma(\Omega_e)$, we multiply the second equation of (1.1) by $\nabla\varphi$ and integrate it in $\Omega \setminus \overline{\Omega_c}$. Using the formula of integration by part, we have

$$\begin{aligned}
&\mathbf{i}\,\omega \int_{\Omega_e} \mu\,(\nabla\psi + \mathbf{H}_s) \cdot \nabla\overline{\varphi} = \mathbf{i}\,\omega \int_{\partial\Omega_e \setminus \partial\Omega} \mu\,(\nabla\psi + \mathbf{H}_s) \cdot \boldsymbol{n}\,\overline{\varphi} \\
&\quad = -\int_{\partial\Omega_e \setminus \Omega} \mathbf{curl}\, \mathbf{E} \cdot \boldsymbol{n}\,\overline{\varphi} = \sum_{i=1}^{I} \int_{\Sigma_i} \mathbf{E} \cdot [\boldsymbol{n} \times \nabla\overline{\varphi}] + \int_{\partial\Omega_c} \mathbf{E} \cdot (\boldsymbol{n} \times \nabla\overline{\varphi}) \\
&\quad = \int_{\partial\Omega_c} \mathbf{E} \cdot (\boldsymbol{n} \times \nabla\overline{\varphi}),
\end{aligned} \tag{2.6}$$

where $\boldsymbol{n}$ is the unit normal vector on $\partial\Omega_e$ pointing to the exterior of Ω_e. On the other hand, integrating the equation in Ω_c leads to

$$\begin{aligned}
&\mathbf{i}\,\omega \int_{\Omega_c} \mu\, \mathbf{H}_0 \cdot \overline{\mathbf{w}} + \int_{\Omega_c} \sigma^{-1} \mathbf{curl}\, \mathbf{H}_0 \cdot \mathbf{curl}\, \overline{\mathbf{w}} \\
&\quad = \int_{\partial\Omega_c} \sigma^{-1} (\mathbf{curl}\, \mathbf{H}_0 \times \boldsymbol{n}) \cdot \overline{\mathbf{w}} - \mathbf{i}\,\omega \int_{\Omega_c} \mu\, \mathbf{H}_s \cdot \overline{\mathbf{w}} \\
&\quad = \int_{\partial\Omega_c} \mathbf{E} \cdot (\boldsymbol{n} \times \overline{\mathbf{w}}) - \mathbf{i}\,\omega \int_{\Omega_c} \mu\, \mathbf{H}_s \cdot \overline{\mathbf{w}},
\end{aligned} \tag{2.7}$$

where $\boldsymbol{n}$ is the unit normal vector on $\partial\Omega_c$ pointing to the exterior of Ω_c. By the tangential continuity of $\mathbf{E}$ and adding (2.6) to (2.7), we have

$$
\begin{aligned}
(2.8)\qquad & \mathbf{i}\,\omega\int_{\Omega_e}\mu\,\nabla\psi\cdot\nabla\overline{\varphi}+\mathbf{i}\,\omega\int_{\Omega_c}\mu\,\mathbf{H}_0\cdot\overline{\mathbf{w}}+\int_{\Omega_c}\sigma^{-1}\mathbf{curl}\,\mathbf{H}_0\cdot\mathbf{curl}\,\overline{\mathbf{w}}\\
&=-\mathbf{i}\,\omega\int_{\Omega}\mu\,\mathbf{H}_s\cdot\overline{\mathbf{v}}+\int_{\partial\Omega_c}\mathbf{E}_t\cdot(\overline{\mathbf{w}}\times\boldsymbol{n}-\nabla\overline{\varphi}\times\boldsymbol{n})\\
&=-\mathbf{i}\,\omega\int_{\Omega}\mu\,\mathbf{H}_s\cdot\overline{\mathbf{v}},
\end{aligned}
$$

where $\boldsymbol{n}$ is the unit outer normal vector of $\partial\Omega_c$ and $\mathbf{E}_t:=(\mathbf{n}\times\mathbf{E})\times\boldsymbol{n}$ is the tangential part of $\mathbf{E}$.

Thanks to (2.8), we obtain the variational problem based on the magnetic field and scalar magnetic potential: Find $\mathbf{u}\in\mathbf{U}$ such that

$$
a(\mathbf{u},\,\mathbf{v})=-\mathbf{i}\,\omega\,(\mu\mathbf{H}_s,\,\mathbf{v}),\quad\forall\,\mathbf{v}\in\mathbf{U}, \tag{2.9}
$$

where the bilinear form is defined by

$$
a(\mathbf{u},\,\mathbf{v}):=\mathbf{i}\,\omega\,(\mu\,\mathbf{u},\,\mathbf{v})+\int_{\Omega_c}\sigma^{-1}\,\mathbf{curl}\,\mathbf{u}\cdot\mathbf{curl}\,\mathbf{v}\,.
$$

THEOREM 2.3. *Let $\mathbf{H}_s\in\mathbf{L}^2(\Omega)$, then problem (2.9) has unique solution $\mathbf{u}\in\mathbf{U}$ and there exists a constant C only depending on Ω and material parameters such that*

$$
\|\mathbf{u}\|_{\mathbf{H}(\mathbf{curl};\,\Omega)}\le C\|\mathbf{H}_s\|_{0,\Omega}.
$$

Proof. The theorem can be proved by similar arguments to the proof of [5, Proposition 8.1]. We omit the proof here. □

3. Finite element approximations. We consider a family of nested regular tetrahedral triangulations of Ω, $\{\mathcal{T}_k\}_{k=0}^{K}$, generated by local refinements. For any mesh $\mathcal{T}_k$, we assume that $\mathcal{T}_k^c:=\mathcal{T}_k|_{\Omega_c}$ and $\mathcal{T}_k^e:=\mathcal{T}_k|_{\Omega_e}$ are triangulations of Ω_c and Ω_e respectively.

Let $V_k\subset H^1(\Omega)$ and $V_k^e\subset H^1(\Omega_e)$ be the conforming linear Lagrangian finite element spaces over $\mathcal{T}_k$ and $\mathcal{T}_k^e$ respectively, and $\mathbf{V}_k^c\subset\mathbf{H}(\mathbf{curl};\,\Omega_c)$ be the Nédélec edge element space of the lowest order over $\mathcal{T}_k^c$ [19]. We introduce the finite element space $\mathbf{U}_k\subset\mathbf{U}$ by

$$
\mathbf{U}_k=\Big\{\mathbf{v}:\ \mathbf{v}=\tilde{\nabla}\varphi\ \text{ in }\Omega\setminus\overline{\Omega_c}\text{ and }\mathbf{v}=\mathbf{w}\text{ in }\Omega_c\text{ such that }\nabla\varphi\times\boldsymbol{n}=\mathbf{w}\times\mathbf{n}\text{ on }\partial\Omega_c,\\
\varphi\in H^1_\Sigma(\Omega_e)\bigcap V_k^e\text{ and }\mathbf{w}\in\mathbf{V}_k^c\Big\}.
$$

The discrete problem on $\mathbf{U}_k$ reads: Find $\mathbf{u}_k\in\mathbf{U}_k$ such that

$$
a(\mathbf{u}_k,\,\mathbf{v}_k)=-\mathbf{i}\,\omega\,(\mu\mathbf{H}_s,\,\mathbf{v}_k),\quad\forall\,\mathbf{v}_k\in\mathbf{U}_k, \tag{3.1}
$$

In the following we are going to explain how to implement the basis functions of $\mathbf{U}_k$ in real computations.

Let $\mathcal{E}_k(D)$ and $\mathcal{V}_k(D)$ be the set of edges and vertices of $\mathcal{T}_k$ contained in some subset $D \subset \Omega$. For any edge $E \in \mathcal{E}_k(\Omega)$, the canonical basis function of the Nédélec edge element space with respect to E is defined by

$$\mathrm{supp}(\mathbf{w}_E) = \bigcup \{\overline{T} :\ E \subset \partial T, T \in \mathcal{T}_k\},$$
$$\mathbf{w}_E = \lambda_2^T \nabla \lambda_1^T - \lambda_1^T \nabla \lambda_2^T \quad \text{in } T \subset \mathrm{supp}(\mathbf{w}_E),$$

where $\lambda_1^T, \ldots, \lambda_4^T$ are barycentric coordinates of T. The nodal edge element interpolation operator Π_k is defined by

$$\Pi_k \mathbf{v} = \sum_{E \in \mathcal{E}_k(\overline{\Omega})} \int_E \mathbf{v} \cdot \boldsymbol{\tau} dE\, \mathbf{w}_E \quad \forall\, \mathbf{v} \in \mathrm{Dom}(\Pi_k). \tag{3.2}$$

Denote by Φ_A the canonical basis function of V_k with respect to $A \in \mathcal{V}_k(\overline{\Omega})$. Clearly the following identity holds

$$\Pi_k(\nabla \Phi_A) = \nabla \Phi_A \quad \forall\, A \in \mathcal{V}_k(\overline{\Omega}).$$

Since the scalar potential is discontinuous across every "cut", we need additional piecewisely defined functions representing these continuities. For each "cut" Σ_i, let q_i be the $H^1(\Omega_e)$-conforming linear finite element function on $\mathcal{T}_0^e$ satisfying

$$[q_i]_{\Sigma_j} = \delta_{ij},\ 1 \le j \le I, \text{ and } q_i(A) = 0, \text{ for any node } A \in \mathcal{V}_0(\overline{\Omega}) \text{ not on } \overline{\Sigma}_i. \tag{3.3}$$

We remark that $\mathbf{U}_k$ can be defined equivalently by

$$\begin{aligned}\mathbf{U}_k = \mathrm{Span}\big\{\mathbf{w}_E,\ E \in \mathcal{E}_k(\Omega_c);\quad \Pi_k(\nabla \Phi_A|_{\overline{\Omega_e}}),\ A \in \mathcal{V}_k\left(\overline{\Omega_e}\right);\\ \Pi_0(\nabla q_i),\ 1 \le i \le I\big\},\end{aligned} \tag{3.4}$$

where $\overline{\Omega_e} = \overline{\Omega} \setminus \Omega_c$ and we extend $\nabla \Phi_A|_{\overline{\Omega_e}}$ and ∇q_i by zero to the interior of Ω_c. In fact, the following theorem indicates that (3.4) defines a good approximation to $\mathbf{U}$.

THEOREM 3.1. *Let $\mathcal{T}_h$ be a quasi-uniform triangulation of Ω and h be the maximal diameter of all elements in $\mathcal{T}_h$. Then for any $\mathbf{v} \in \mathbf{U}$,*

$$\lim_{h \to 0} \min_{\mathbf{v}_h \in \mathbf{U}_h} \|\mathbf{v} - \mathbf{v}_h\|_{\mathbf{H}(\mathbf{curl};\Omega)} = 0.$$

Proof. In this proof, all notation with subscript h have similar meanings to those with subscript k in the preceding part.

To begin, by using Theorem 3.3, we split every $\mathbf{v} \in \mathbf{U}$ into

$$\mathbf{v} = \nabla v + \mathbf{v}_0 + \mathbf{v}_s \quad v \in H^1(\Omega),\ \mathbf{v}_0 \in \mathbf{U}_h,\ \mathbf{v}_s \in \mathbf{H}_0^1(\Omega_c),$$
$$\|v\|_{H^1(\Omega)} + \|\mathbf{v}_0\|_{\mathbf{H}(\mathbf{curl};\Omega)} + \|\mathbf{v}_s\|_{\mathbf{H}(\mathbf{curl};\Omega_c)} \le C\, \|\mathbf{v}\|_{\mathbf{H}(\mathbf{curl};\Omega)},$$

where C only depends on Ω_e and the initial mesh $\mathcal{T}_0$. Thus we only need to prove

$$\lim_{h \to 0} \min_{\mathbf{v}_h \in \mathbf{U}_h} \|\mathbf{v}_h - \nabla v - \mathbf{v}_s\|_{\mathbf{H}(\mathbf{curl};\Omega)} = 0.$$

For any $\epsilon > 0$, by the density of $C^\infty(\bar{\Omega})$ in $H^1(\Omega)$ and $\mathbf{C}_0^\infty(\Omega_c)$ in $\mathbf{H}_0^1(\Omega_c)$, there exist $v_\infty \in C^\infty(\bar{\Omega})$ and $\mathbf{v}_\infty \in \mathbf{C}_0^\infty(\Omega_c)$ such that

$$\|v - v_\infty\|_{1,\Omega} + \|\mathbf{v}_s - \mathbf{v}_\infty\|_{\mathbf{H}(\mathbf{curl};\,\Omega_c)} < \epsilon.$$

Note that the linear Lagrangian element interpolation $\mathcal{L}_h v_\infty$ and the Nédélec edge element interpolation $\Pi_h \mathbf{v}_\infty$ belong to $\mathbf{U}_h$. We find

$$\lim_{h\to 0} \min_{\mathbf{v}_h\in\mathbf{U}_h} \|\mathbf{v}_h - \nabla v - \mathbf{v}_s\|_{\mathbf{H}(\mathbf{curl};\Omega)} < \epsilon.$$

The arbitrariness of ϵ concludes the proof. ◻

The above theorem merely claim that we have chosen the right finite element space. But due to the poor regularity of the solution $\mathbf{u}$, we cannot afford uniform mesh refinement. This justifies the necessity of adaptive mesh refinements.

To end this section, we are going to prove the Hemholtz-type decomposition of $\mathbf{U}$. Hemholtz-type decompositions are frequently used in theoretical and numerical analyses of Maxwell's equations. To define a bounded finite element interpolation operator on $\mathbf{H}(\mathbf{curl};\Omega)$, we need to decompose every function in $\mathbf{H}(\mathbf{curl};\Omega)$ into the sum of an irrotational part and an H^1-smooth part and deal with them in the policy of "divide and conquer".

Theorem 3.2. [11] *If $\mathcal{D}$ is a bounded Lipschitz domain, the following space decomposition is stable in the norm of $\mathbf{H}(\mathbf{curl};\,\mathcal{D})$:*

$$\mathbf{H}_0(\mathbf{curl};\,\mathcal{D}) = \nabla H_0^1(\mathcal{D}) + \mathbf{H}_0^1(\mathcal{D}). \tag{3.5}$$

In the next, we will introduce a decomposition of $\mathbf{U}$. Since both Ω_c and $\Omega\setminus\overline{\Omega_c}$ are multiply connected, it is difficult to find a scalar function ψ with constant jumps across all "cuts" to define the irrotational part. In stead, we introduce a finite element function to deal with these discontinuities.

Theorem 3.3. *Let $\mathcal{T}_0$ be the initial regular triangulation of Ω and $\mathbf{U}_0$ be the finite element space with respect to $\mathcal{T}_0$. The following decomposition of spaces is stable:*

$$\mathbf{U} = \nabla H^1(\Omega) + \mathbf{U}_0 + \mathbf{H}_0^1(\Omega_c), \tag{3.6}$$

where the functions in $\mathbf{H}_0^1(\Omega_c)$ are understood to vanish outside Ω_c.

Proof. By the definition of $\mathbf{U}$, for any function $\mathbf{v}\in\mathbf{U}$, there exists a $\varphi_e \in H^1_\Sigma(\Omega_e)/\mathbb{R}^1$ such that $\mathbf{v} = \tilde{\nabla}\varphi_e$ in $\Omega\setminus\overline{\Omega_c}$. We define

$$\varphi_0 := \sum_{i=1}^{I} [\varphi_e]_{\Sigma_i}\, q_i \quad \text{and} \quad \mathbf{v}_0 := \Pi_0(\tilde{\nabla}\varphi_0), \tag{3.7}$$

where Π_0 is the nodal edge element interpolation in (3.2) which are defined on $\mathcal{T}_0$. In view that

$$|[\varphi_e]_{\Sigma_i}| = \frac{1}{|\Sigma_i|}\int_{\Sigma_i} |[\varphi_e]_{\Sigma_i}| \le C\|\varphi_e\|_{1,\Omega_e} \quad 1\le i\le I,$$

there exists a constant C depending on $\mathcal{T}_0$ and Ω_e such that

$$\|\varphi_0\|_{1,\Omega_e} \le C\|\varphi_e\|_{1,\Omega_e} \quad \text{and} \quad \|\mathbf{v}_0\|_{\mathbf{H}(\mathbf{curl};\,\Omega)} \le C\|\varphi_e\|_{1,\Omega_e}. \tag{3.8}$$

It is easy to see $\varphi_e - \varphi_0 \in H^1(\Omega\setminus\overline{\Omega_c})$. By Stein's extension theorem [22, Theorem 5, page 181] and (3.8), there exists an extension of $\varphi_e-\varphi_0$ denoted by $\varphi_{e0}\in H^1(\Omega)/\mathbb{R}^1$ such that

$$\varphi_{e0} = \varphi_e - \varphi_0, \quad \text{in } \Omega\setminus\overline{\Omega_c}, \tag{3.9}$$

$$\|\varphi_{e0}\|_{1,\Omega} \le C\|\varphi_e-\varphi_0\|_{1,\Omega\setminus\overline{\Omega_c}} \le C\|\varphi_e\|_{1,\Omega_e} \le C\|\nabla\varphi_e\|_{0,\Omega_e}. \tag{3.10}$$

Now (3.7) and (3.9) indicate $\mathbf{v} - \nabla\varphi_{e0} - \mathbf{v}_0 \in \mathbf{H}_0(\mathrm{curl}; \Omega_c)$. By Theorem 3.2, there exist $p \in H_0^1(\Omega_c)$ and $\mathbf{v}_s \in \mathbf{H}_0^1(\Omega_c)$ such that

$$\mathbf{v} - \nabla\varphi_{e0} - \mathbf{v}_0 = \nabla p + \mathbf{v}_s, \quad \text{in } \Omega_c, \tag{3.11}$$

$$\|p\|_{1,\Omega_c} + \|\mathbf{v}_s\|_{1,\Omega_c} \le C\|\mathbf{v} - \nabla\varphi_{e0} - \mathbf{v}_0\|_{\mathbf{H}(\mathbf{curl};\,\Omega_c)} \le C\|\mathbf{v}\|_{\mathbf{H}(\mathbf{curl};\,\Omega)}. \tag{3.12}$$

Extend p and $\mathbf{v}_s$ by zero to the exterior of Ω_c and still denote the extensions by p and $\mathbf{v}_s$. It follows that

$$\mathbf{v} = \nabla(\varphi_{e0} + p) + \mathbf{v}_0 + \mathbf{v}_s \quad \text{in } \Omega_c.$$

In view of (3.8), (3.10), and (3.12), this yields the desired stable decomposition. $\square$

4. Residual based a posteriori error estimators. Unless otherwise stated, we assume that the generic constant C only depends on Ω, material parameters μ and σ, and the initial mesh $\mathcal{T}_0$ in the rest of this paper. For the sake of convenience, we neglect iterative errors in real computations.

Let $\mathbf{u}$ and $\mathbf{u}_k$ be the solutions of (2.9) and (3.1) respectively. The total error is defined by $\mathbf{e}_k := \mathbf{u} - \mathbf{u}_k$. By Theorem 3.3, there exist $\phi \in H^1(\Omega)$, $\mathbf{e}_0 \in \mathbf{U}_0$, and $\mathbf{e}_s \in \mathbf{H}_0^1(\Omega_c)$ such that

$$\mathbf{e}_k = \nabla\phi + \mathbf{e}_0 + \mathbf{e}_s, \tag{4.1}$$

$$\|\phi\|_{1,\Omega} + \|\mathbf{e}_0\|_{\mathbf{H}(\mathbf{curl};\,\Omega)} + \|\mathbf{e}_s\|_{1,\Omega} \le C\|\mathbf{e}_k\|_{\mathbf{H}(\mathbf{curl};\,\Omega)}. \tag{4.2}$$

Multiply both sides of (2.9) by $1 - \mathbf{i}$, we have

$$\|\mathbf{e}_k\|^2_{\mathbf{H}(\mathbf{curl};\,\Omega)} \le C\,\mathrm{Re}\{(1-\mathbf{i})\,a(\mathbf{e}_k,\,\mathbf{e}_k)\} \le C|a(\mathbf{e}_k,\,\nabla\phi)| + C|a(\mathbf{e}_k,\,\mathbf{e}_s)|, \tag{4.3}$$

wherein we have used the Galerkin orthogonality $a(\mathbf{e}_k,\,\mathbf{e}_0) = 0$.

To deduce the a posteriori error estimate, we introduce the Scott-Zhang Operator $\mathcal{I}_k$[21] : $H^1(\Omega) \to V_k$ and the BHHW-Operator Λ_k[4] : $\mathbf{H}_0^1(\Omega_c) \to \mathbf{V}_k^c$, which satisfy the following approximation and stability properties: for any $\phi_h \in V_k$, $\phi \in H^1(\Omega)$, $\mathbf{w}_h \in \mathbf{U}_k$, and $\mathbf{w} \in \mathbf{H}_0^1(\Omega_c)$,

$$\begin{cases} \mathcal{I}_k\phi_h = \phi_h, \\ \|\nabla\mathcal{I}_k\phi\|_{0,T} \le C\,|\phi|_{1,D_T}, \\ \|\phi - \mathcal{I}_k\phi\|_{0,T} \le C\,h_T\,|\phi|_{1,D_T}, \\ \|\phi - \mathcal{I}_k\phi\|_{0,F} \le C\,h_F^{1/2}\,|\phi|_{1,D_F}, \end{cases} \tag{4.4}$$

$$\begin{cases} \Lambda_k\mathbf{w}_h = \mathbf{w}_h, \\ \|\Lambda_k\mathbf{w}\|_{\mathbf{H}(\mathbf{curl};\,T)} \le C\,\|\mathbf{w}\|_{1,D_T}, \\ \|\mathbf{w} - \Lambda_k\mathbf{w}\|_{0,T} \le C\,h_T\,|\mathbf{w}|_{1,D_T}, \\ \|\mathbf{w} - \Lambda_k\mathbf{w}\|_{0,F} \le C\,h_F^{1/2}\,|\mathbf{w}|_{1,D_F}, \end{cases} \tag{4.5}$$

where D_A is the union of elements in $\mathcal{T}_k$ with non-empty intersection with A, $A = T$ or F.

LEMMA 4.1. *There exists a positive constant C such that*

$$|a(\mathbf{e}_k, \nabla\varphi)| \le C\|\mathbf{e}_k\|_{\mathbf{H}(\mathbf{curl};\,\Omega)}\Big(\sum_{T\in\mathcal{T}_k}\eta^2_{0,T} + \sum_{F\in\mathcal{F}_k(\Omega)}\eta^2_{0,F} + \sum_{F\in\mathcal{F}_k(\partial\Omega)}\eta^2_{0,B,F}\Big)^{1/2}, \tag{4.6}$$

where $\mathcal{F}_k(D)$ *is the set of edges contained in* D*,* $D = \Omega, \partial\Omega$*, and*

$$\begin{aligned}\eta_{0,T} &:= \omega h_T \left\|\mathrm{div}(\mu\,\mathbf{H}_s + \mu\,\mathbf{u}_k)\right\|_{0,T}, \\ \eta_{0,F} &:= \omega\sqrt{h_F}\,\left\|[\mu\,\mathbf{H}_s + \mu\,\mathbf{u}_k]_F\cdot\boldsymbol{n}\right\|_{0,F}, \\ \eta_{0,B,F} &:= \omega\sqrt{h_F}\,\left\|(\mu\,\mathbf{H}_s + \mu\,\mathbf{u}_k)\cdot\boldsymbol{n}\right\|_{0,F}.\end{aligned}$$

Proof. By (2.9) and the formula of integration by part, we have

$$\begin{aligned}a(\mathbf{e}_k, \nabla\varphi) = a(\mathbf{e}_k, \nabla\varphi - \nabla\mathcal{I}_k\varphi) &= \mathbf{i}\,\omega(\mu\,\mathbf{H}_s + \mu\,\mathbf{u}_k,\, \nabla\mathcal{I}_k\varphi - \nabla\varphi) \\ &= \mathbf{i}\,\omega\sum_{T\in\mathcal{T}_k}\int_T \mathrm{div}(\mu\,\mathbf{H}_s + \mu\,\mathbf{u}_k)\,(\varphi - \mathcal{I}_k\varphi) \\ &\quad + \mathbf{i}\,\omega\sum_{F\in\mathcal{F}_k(\Omega)}\int_F [\mu\,\mathbf{H}_s + \mu\,\mathbf{u}_k]_F\cdot\boldsymbol{n}\,(\mathcal{I}_k\varphi - \varphi) \\ &\quad + \mathbf{i}\,\omega\sum_{F\in\mathcal{F}_k(\partial\Omega)}\int_F (\mu\,\mathbf{H}_s + \mu\,\mathbf{u}_k)\cdot\boldsymbol{n}\,(\mathcal{I}_k\varphi - \varphi).\end{aligned}$$

In view of (4.4), we complete the proof by using Schwartz's inequality. ∎

LEMMA 4.2. *There exists a positive constant* C *such that*

$$|a(\mathbf{e}_k,\,\mathbf{e}_s)| \le C\|\mathbf{e}_k\|_{\mathbf{H}(\mathbf{curl};\,\Omega)}\Big(\sum_{T\in\mathcal{T}_k^c}\eta_{1,T}^2 + \sum_{F\in\mathcal{F}_k(\Omega_c)}\eta_{1,F}^2\Big)^{1/2}, \tag{4.7}$$

where

$$\begin{aligned}\eta_{1,F} &:= \sqrt{h_F}\,\left\|\left[\sigma^{-1}\mathbf{curl}\,\mathbf{u}_k\times\boldsymbol{n}\right]_{J,F}\right\|_{0,F}, \\ \eta_{1,T} &:= h_T\left\|\mathbf{i}\,\omega\,\mu\,(\mathbf{H}_s + \mathbf{u}_k) + \mathbf{curl}(\sigma^{-1}\,\mathbf{curl}\,\mathbf{u}_k)\right\|_{0,T}.\end{aligned}$$

Proof. By the Galerkin orthogonality and (2.9), we have

$$\begin{aligned}a(\mathbf{e}_k,\,\mathbf{e}_s) = a(\mathbf{e}_k,\,\mathbf{e}_s - \Lambda_k\mathbf{e}_s) &= \mathbf{i}\,\omega\int_\Omega \mu\,\mathbf{H}_s\cdot(\Lambda_k\mathbf{e}_s - \mathbf{e}_s) + a(\mathbf{u}_k, \Lambda_k\mathbf{e}_s - \mathbf{e}_s) \\ &= \sum_{T\in\mathcal{T}_k^c}\int_T\left\{\mathbf{i}\,\omega\,\mu\,(\mathbf{H}_s + \mathbf{u}_k) + \mathbf{curl}(\sigma^{-1}\,\mathbf{curl}\,\mathbf{u}_k)\right\}\cdot(\Lambda_k\mathbf{e}_s - \mathbf{e}_s) \\ &\quad + \sum_{F\in\mathcal{F}_k^{\Omega_c}}\int_F\left[\sigma^{-1}\,\mathbf{curl}\,\mathbf{u}_k\times\boldsymbol{n}\right]_F\cdot(\mathbf{e}_s - \Lambda_k\mathbf{e}_s).\end{aligned}$$

We finish the proof by (4.5) and Schwartz's inequality. ∎

We remark that $\eta_{1,T}$ and $\eta_{0,T}$ are respectively the residuals of the second and third equations of (1.1), $\eta_{1,F}$ and $\eta_{0,F}$ reflect the interface conditions of the electric field and the magnetic flux respectively, $\eta_{0,B,F}$ is the boundary residual of (2.5). In view of Lemma 4.1 and 4.2, we have actually proved the following upper bound estimate:

THEOREM 4.3. *There exists a generic positive constant* C *depending only on* Ω*, the initial mesh* $\mathcal{T}_0$*, and material parameters* μ*,* σ *such that*

$$\|\mathbf{e}_k\|_{\mathbf{H}(\mathbf{curl};\,\Omega)} \le C\,\eta_k, \tag{4.8}$$

where the a posteriori error estimate η_k is defined by

$$\eta_k^2 := \sum_{T\in\mathcal{T}_k} \eta_{0,T}^2 + \sum_{F\in\mathcal{F}_k(\Omega)} \eta_{0,F}^2 + \sum_{F\in\mathcal{F}_k(\partial\Omega)} \eta_{0,B,F}^2 + \sum_{T\in\mathcal{T}_k^c} \eta_{1,T}^2 + \sum_{F\in\mathcal{F}_k(\Omega_c)} \eta_{1,F}^2. \tag{4.9}$$

Let $\mathcal{Q}_D$: $\mathbf{L}^2(D) \to \mathbf{P}_1(D)$ be the $\mathbf{L}^2$-projection, $\mathcal{Q}_{\rm div}^F$: $\mathbf{H}(\mathrm{div};\, D) \to \mathbf{P}_1(D)$ be the $\mathbf{H}(\mathrm{div})$-projection with $\|\cdot\|^2_{\mathbf{H}(\mathrm{div};D)} := \|\cdot\|^2_{\mathbf{L}^2(D)} + \|\mathrm{div}\,\cdot\|^2_{\mathbf{L}^2(D)}$, where $\mathbf{P}_1(D)$ is the space of linear vector polynomials defined on D. To insure the efficiency of a posteriori error estimators on the righthand side of (4.9), we obtain the lower bound by similar arguments to those in [4].

THEOREM 4.4. *There exists a generic positive constant C depending only on Ω, the initial mesh $\mathcal{T}_0$, and material parameters μ and σ such that*

$$\begin{aligned}\eta_k^2 \le C\Big\{ &\|\mathbf{e}_k\|^2_{\mathbf{H}(\mathbf{curl};\,\Omega)} + \omega^2 \sum_{F\in\mathcal{F}_k(\overline{\Omega})} h_F \left\|(I-\mathcal{Q}_F)\left[\mu\mathbf{H}_s\cdot\boldsymbol{n}\right]_F\right\|^2_{0,F} \\ &+\omega^2 \sum_{T\in\mathcal{T}_k} h_T^2 \|(I-\mathcal{Q}_T)\mathrm{div}(\mu\mathbf{H}_s)\|^2_{0,T} + \omega^2 \sum_{T\in\mathcal{T}_k^c} h_T^2 \|(I-\mathcal{Q}_T)(\mu\mathbf{H}_s)\|^2_{0,T}\Big\}.\end{aligned} \tag{4.10}$$

REMARK 4.5. *The last three terms on the righthand side of (4.10) embody the oscillation of known information $\mu\mathbf{H}_s$ on the current mesh. They are higher order terms compared with η_k if $\mu\mathbf{H}_s$ is element-wisely smooth and normally continuous across all faces.*

5. Numerical results. In the adaptive algorithm, we control the mesh refinements by the error estimate η_k defined in Theorem 4.3. The implementation of our algorithm is based on the adaptive finite element package ALBERT [20] and carried out on Origin 3800.

In the following, we report two numerical experiments to demonstrate the competitive performance of the proposed method.

EXAMPLE 5.1. We consider the real-valued problem: Find $\mathbf{u} \in \mathbf{U}$ such that

$$\int_\Omega \alpha\,\mathbf{u}\cdot\mathbf{v} + \int_{\Omega_c} \mathbf{curl}\,\mathbf{u}\cdot\mathbf{curl}\,\mathbf{v} = \int_\Omega \mathbf{f}\cdot\mathbf{v} \quad \forall\,\mathbf{v}\in\mathbf{U},$$

where $\mathbf{f} = (1,1,1)^T$, $\alpha = 1000$ in Ω_c and $\alpha = 1$ elsewhere, $\Omega = (0,\ 1)^3$, $\Omega_c = D \times \{(0.2,\ 0.4) \cup (0.6,\ 0.8)\}$ with $D = (0.2,\ 0.8)^2 \setminus [0.4,\ 0.6]^2$ (see Fig. 5.1).

Fig.5.2 shows the curve of $\log \eta_k$ versus $\log N_k$, where N_k is the number of elements in $\mathcal{T}_k$. It indicates that the adaptive mesh and the associated numerical complexity are quasi-optimal, i.e.

$$\eta_k \approx C\,N_k^{-1/3}. \tag{5.1}$$

It also shows that adaptive mesh refinements are obviously superior to uniform mesh refinements.

EXAMPLE 5.2. The second experiment is a benchmark problem in electrical engineering — the Team Workshop Problem 7. This problem consists of an aluminum plate with a hole above which a racetrack shaped coil is placed (see Fig.5.3). The aluminum plate has a conductivity of 3.526×10^7 S/m and the sinusoidal driving current of the coil is 2742 AT. The frequency of the driving current is $\omega = 2\pi \times 50$ Hz.

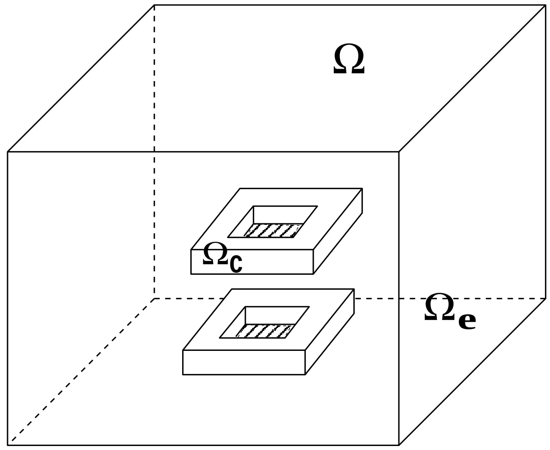

FIG. 5.1. *Multiply connected Ω_c for Example 5.1.*

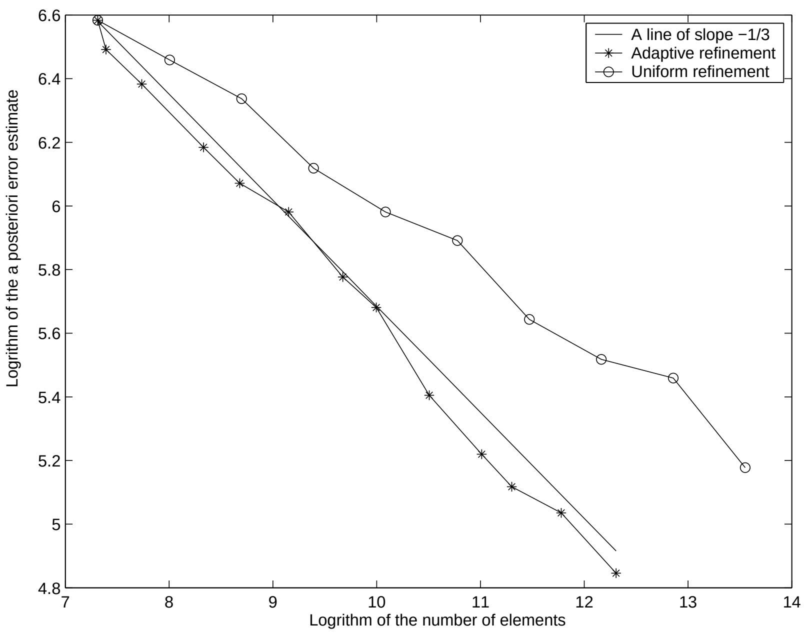

FIG. 5.2. *Quasi-optimality of the adaptive mesh refinements of the a posteriori error estimate (Example 5.1).*

We set Ω to be a cubic domain with one-meter edges and compare the numerical values of the vertical magnetic flux $B_z = \mu H_z$ with measured values on some points, where H_z is the third component of $\mathbf{H} = \mathrm{Re}(\mathbf{u}_k + \mathbf{H}_s)$ and $\mathbf{u}_k$ is the solution of (3.1). These points are located at $y = 72\,\mathrm{mm}$, $z = 34\,\mathrm{mm}$, and $x = (18 \times i)\,\mathrm{mm}$ where $i = 0, \cdots, 16$ (see Fig. 5.3).

Fig.5.4 shows the curve of $\log \eta_k$ versus $\log N_k$. It indicates that the adaptive method based on the a posteriori error estimates satisfies the very desirable quasi-optimality property in (5.1).

Fig.5.5 – 5.7 show the numerical values of B_z by adaptive finite element method.

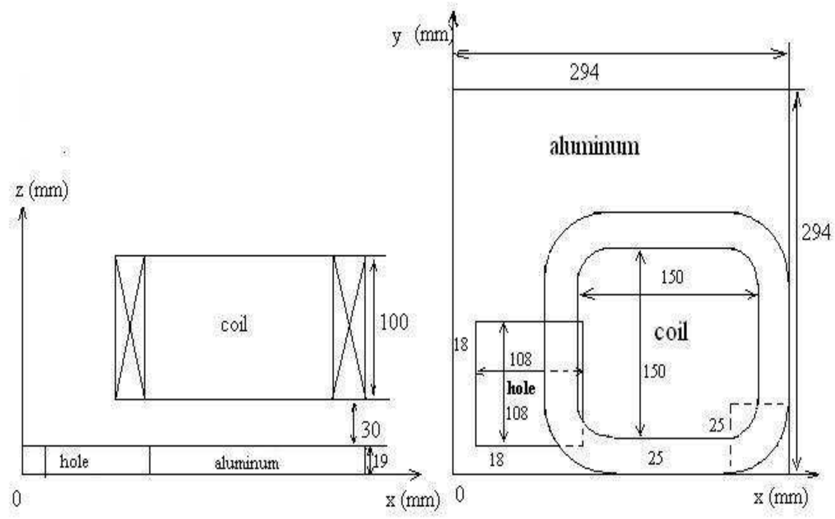

FIG. 5.3. *The geometry of Team Workshop Problem 7 in frontal view with specified positions. All geometry dimensions are given in mm.*

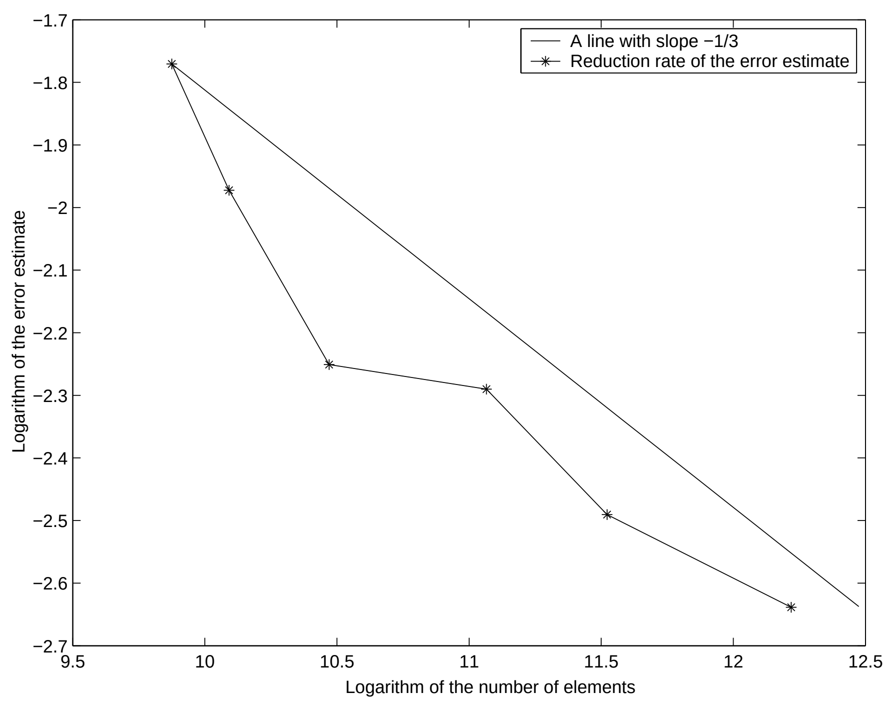

FIG. 5.4. *Quasi-optimality of the adaptive mesh refinements of the total a posteriori error estimate (Example 5.2).*

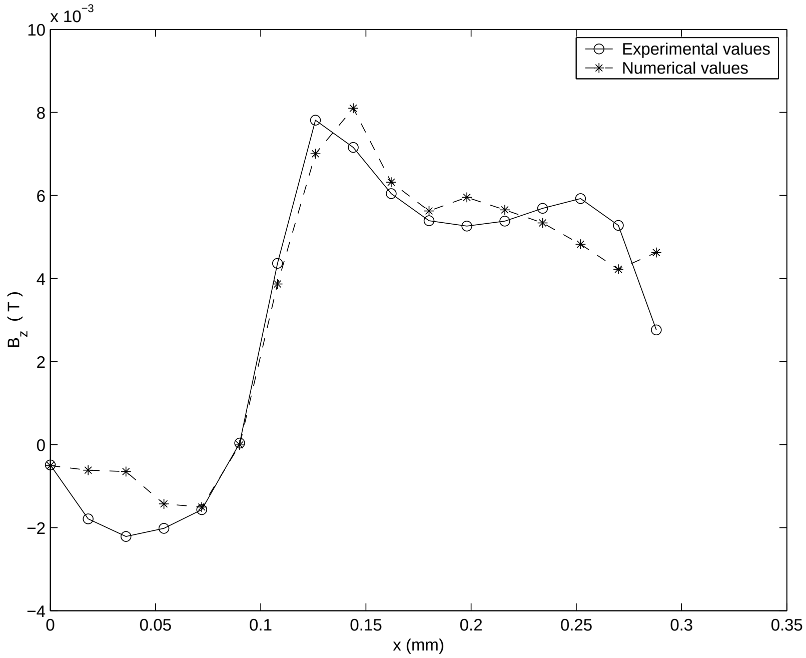

FIG. 5.5. *Numerical values of μH_z on an adaptive mesh with the number of degrees of freedom being 19,762 (Example 5.2).*

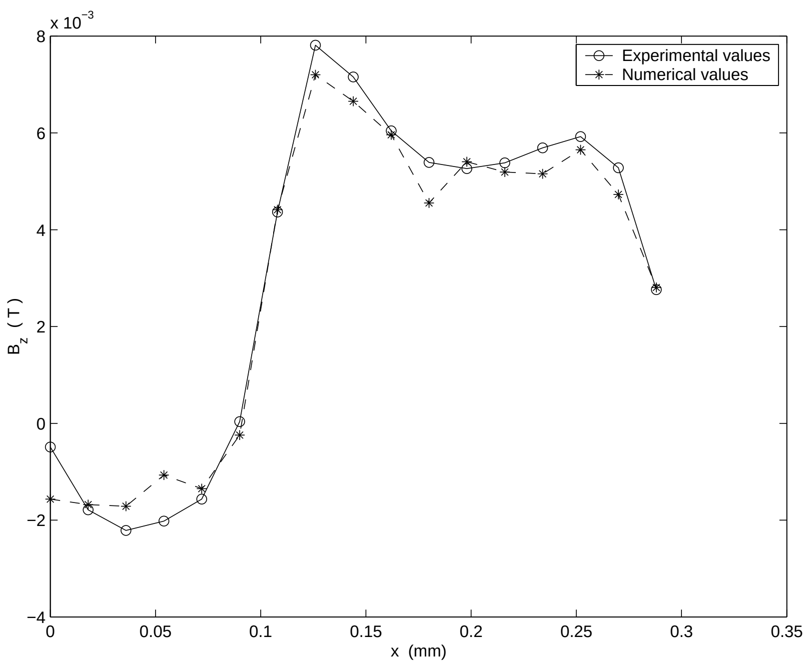

FIG. 5.6. *Numerical values of μH_z on an adaptive mesh with the number of degrees of freedom being 32,851 (Example 5.2).*

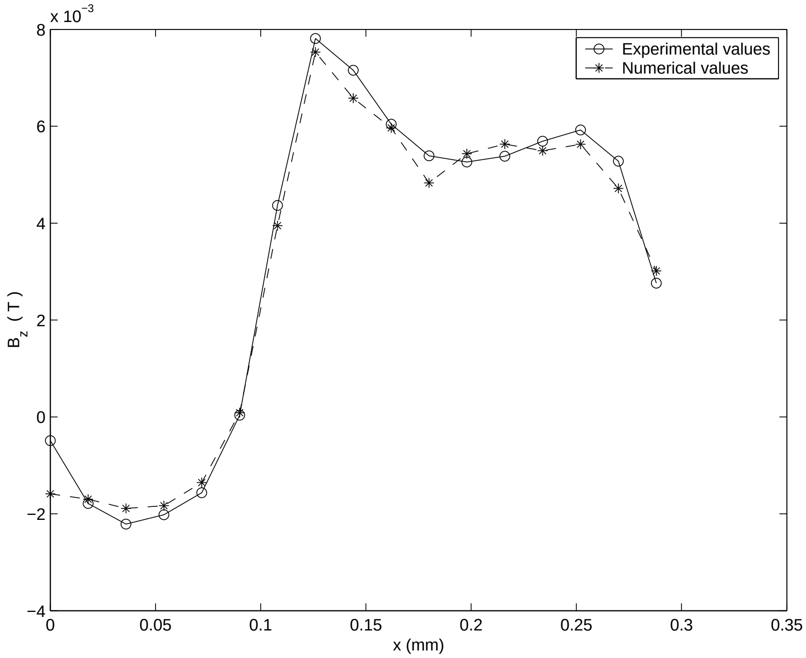

Fig. 5.7. *Numerical values of μH_z on an adaptive mesh with the number of degrees of freedom being 71,201 (Example 5.2).*

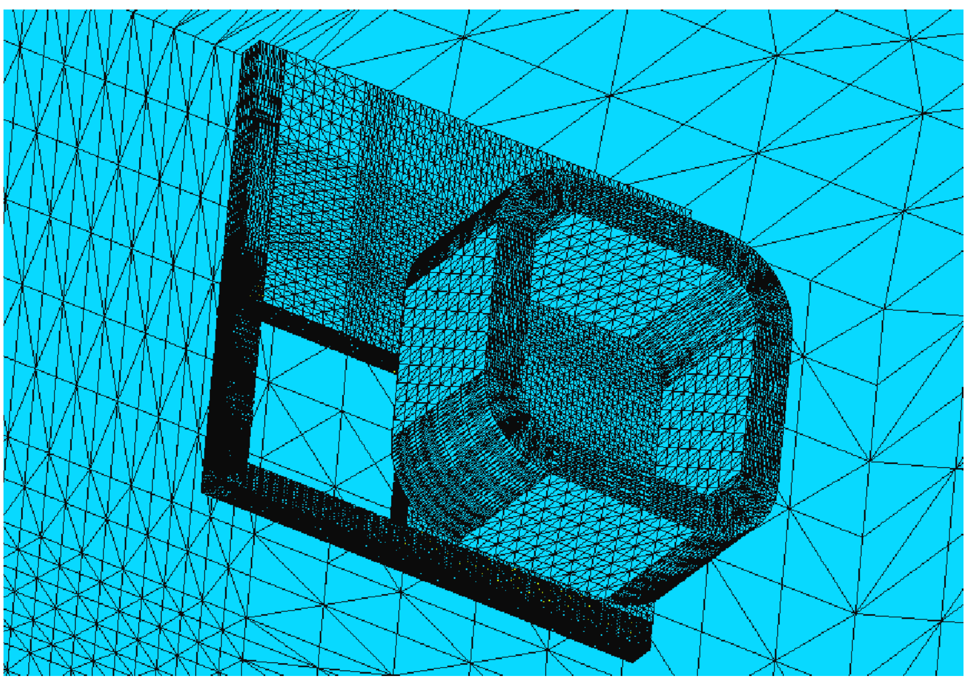

Fig. 5.8. *An adaptively refined mesh of 202,640 elements after 6 adaptive iterations from 19,440 initial elements (Example 5.2).*

With the number of degrees of freedom increasing, the agreement with experimental values become better and better.

Fig. 5.8 shows an adaptively refined mesh of 202,640 elements after 6 adaptive iterations from 19,440 initial elements. We observe that the mesh is locally refined on the surface of the conductor.

Acknowledgement. The authors would like to thank the referees for their careful reading of the paper and valuable comments and suggestions.

REFERENCES

[1] H. Ammari, A. Buffa, and J.C. Nédélec, *A justification of eddy current model for the Maxwell equations*, SIAM J. APPL. MATH., Vol. 60(2000), pp.1805-1823.

[2] C. Amrouche, C. Bernardi, M. Dauge, and V.Girault, *Vector potentials in three-dimensional non-smooth domains*, Math. Meth. Appl. Sci., Vol. 21(1998), pp. 823-864.

[3] I. Babuška and C. Rheinboldt, *Error estimates for adaptive finite element computations*, SIAM J. Numer. Anal., 15(1978).

[4] R. Beck, R. Hiptmar, R.H.W. Hoppe, and B. Wohlmuth, *Residual based a posteriori error estimations for eddy current computation*, M2AN Math. Modeling and Numer. Anal. Vol. 34(2000), pp. 159-182.

[5] A. Bossavit, *Computational Electromagnetism, Variational Formulations, Edge Elements, Complementarity*, Academic Press, Boston, 1998.

[6] F. Bouillault, Z. Ren, and A. Razek, *Calculation of eddy currents in an asymmetrical conductor with a hole*, COMPEL, 9(1990), Supplement A, pp. 227-229.

[7] Z. Chen and S. Dai, *On the efficiency of adaptive finite element methods for elliptic problems with discontinuous coefficients*, SIAM J. Sci. Comput., 24(2002), pp. 443-462.

[8] Z. Chen and S. Dai, *Adaptive Galerkin method with error control for a dynamical Ginzburg-Landau model in superconductivity* , SIAM J. Numer. Anal., 38(2001), pp. 1961-1985.

[9] Z. Chen and F. Jia, *An adaptive finite element method with reliable and efficient error control for linear parabolic problems*, Math. Comp. Vol. 73(2004), pp. 1163-1197.

[10] Z. Chen, R.H. Nochetto, and A. Schmidt, *An adaptive finite element method with error control for the continuous casting problem*, Computer Meth. Appl. Mech. Engrg., 189(2000), pp. 249-276.

[11] Z. Chen, L. Wang, and W. Zheng, *An adaptive finite element method for Maxwell's equations with singularities*, SIAM J. Sci. Comput., 29 (2007), pp. 118-138.

[12] Z. Chen and H. Wu, *An adaptive finite element method with perfectly matched absorbing layers for the wave scattering by periodic structures*, SIAM J. Numer. Anal., 41(2003), pp. 799-826.

[13] M. Clemens and T. Weiland, *Transient eddy-current calculations with the FI-method*, IEEE Trans. Magn., Vol. 35(1999), pp. 1163-1166.

[14] M. Costabel, M. Dauge, and S. Nicaise, *Singularities of eddy current problems*, ESAIM: Mathematical Modelling and Numerical Analysis, 37(2003), pp. 807-831.

[15] K. Fujiwara and T. Nakata, *Results for benchmark problem 7 (a symmetrical conductor with a hole)*, COMPEL – The International Journal for Computation and Mathematics in Electrical and Electric Engineering, Vol. 9(1990), pp. 137-154.

[16] P.Dular, F. Henrotte, F. Robert, A. Genon, and W. Legros, *A generalized source magnetic field calculation method for inductors of any shape*, IEEE Trans. Mag., Vol. 33(1997), pp. 1398-1401.

[17] P. Monk, *A posteriori error indicators for Maxwell's equations*, J. Comp. Appl. Math., 100(1998), pp. 173-190.

[18] P. Morin, R.H. Nochetto, and K.G. Siebert, *Data oscillations and convergence of adaptive FEM*, SIAM J. Numer. Anal., 38(2000), pp. 466-488.

[19] J.C. Nédélec, *Mixed finite elements in* $\mathbb{R}^3$, Numer. Math., Vol. 35(1980), pp. 315-341.

[20] A. Schmidt and K.G. Siebert, *ALBERT – An adaptive hierarchical finite element toolbox*, the new version ALBERTA is available online from http://www.alberta-fem.de .

[21] L.R. Scott and S. Zhang, *Finite element interpolation of nonsmooth functions satisfying boundary conditions*, Math. Comp., Vol. 54(1990), pp. 483-493.

[22] E.M. Stein, *Singular Integrals and Differetiability Properties of Functions*, Princeton University Press, Princeton, New Jersey, 1970.

[23] O. Sterz, A. Hauser, and G. Wittum, *Adaptive local multigrid methods for solving time-*

harmonic eddy-current problems, IEEE Transactions on Magnetics, Vol. 42(2006), pp. 309 - 318.

[24] R. Verfürth, *A Review of A Posteriori Error Estimation and Adaptive Mesh-Refinement Rechniques*, Wiley-Teubner, CHichester, Stuttgart, 1996.

[25] W. Zheng, Z. Chen, and L. Wang, *An adaptive finite element method for the $H-$ formulation of time-dependent eddy current problems*, Numer. Math., 103 (2006), pp. 667-689.